COPYRIGHT NOTICE

Investigation on the fiber based approach to estimate the axial load carrying capacity of the circular concrete filled steel tube (CFST)

IOP Conf. Series: Materials Science and Engineering **267** (2017) 012017 doi:10.1088/1757-899X/267/1/012017

Investigation on the fiber based approach to estimate the axial load carrying capacity of the circular concrete filled steel tube (CFST)

B Piscesa[*1,2], **M M Attard**[2], **P Suprobo**[1], **A K Samani**[3]
[1] Civil Engineering Department, Institut Teknologi Sepuluh Nopember, Surabaya 60111, East Java, Indonesia
[2] School of Civil Engineering, University of New South Wales, Sydney NSW 2052, Australia
[3] School of Civil Engineering and Information Technology, Federation University, Ballarat, VIC 3350, Australia

E-mail: piscesa@ce.its.ac.id and bambang.piscesa@live.com

Abstract. External confining devices are often used to enhance the strength and ductility of reinforced concrete columns. Among the available external confining devices, steel tube is one of the most widely used in construction. However, steel tube has some drawbacks such as local buckling which needs to be considered when estimating the axial load carrying capacity of the concrete-filled-steel-tube (CFST) column. To tackle this problem in design, Eurocode 4 provided guidelines to estimate the effective yield strength of the steel tube material. To study the behavior of CFST column, in this paper, a non-linear analysis using a fiber-based approach was conducted. The use of the fiber-based approach allows the engineers to predict not only the axial load carrying capacity but also the complete load-deformation curve of the CFST columns for a known confining pressure. In the proposed fiber-based approach, an inverse analysis is used to estimate the constant confining pressure similar to design-oriented models. This paper also presents comparisons between the fiber-based approach model with the experimental results and the 3D non-linear finite element analysis.

1. Introduction

In the regions with high seismic activities, the design of structures shall comply with rigorous strength and ductility requirements. For instance, the location, the pattern of formation, as well as the behavior of plastic hinges during earthquakes should be well predicted and designed to avoid any brittle failure and sudden collapse of the whole structure. In designing lateral force resisting systems, each structural element should have sufficient strength and ductility to withstand and absorb seismic induced actions in addition to other existing loads. It is important to note that during a major earthquake, the structural elements also experience plastic deformation and damage. The damage in concrete structural elements clearly show a sign of stiffness degradations. Hence, it is important to ensure stiffness degradations and reduction in capacity of concrete elements are gradual and to avoid any sudden capacity loss (due cover spalling or shear failure) of the structural elements.

In the high-rise building, high-strength concrete (HSC) material has become widely popular due to several advantages. By using HSC material, the dimensions of the column can be reduced and thus

increase the usable floor area as well as reducing the concrete material usage (1). However, the behavior of HSC columns is different to the behavior of NSC columns and requires further consideration in design. High-strength concrete has more brittle behavior than normal strength concrete (NSC). Hence, the columns built of HSC are less ductile compared to the columns built from NSC. Furthermore, premature cover spalling has been observed in all tests of RC columns made of HSC material. The premature cover spalling results in a sudden drop in strength. Further, in many cases, these columns cannot reach the code predicted strength. Proper detailing of HSC columns will increase their ductility and the strength of the confined concrete core. However, from the experimental investigation (2, 3), it was found that in most cases, the strength recovery due to the confinement of concrete core still does not compensate the cover spalling and the peak strengths are lower than the code predictions.

One of the efficient ways to avoid cover spalling in HSC RC columns and to improve the ductility of these columns is to provide additional external confinement by FRP wrap or steel tube. In this paper, the focus is limited to the mechanical performance of the concrete-filled-steel-tube or CFST column. CFST columns are very convenient construction method. The steel tubes can act as lost formwork while they enhance the strength and ductility of the concrete core as well as circumventing premature cover spalling. In the design of CFST columns, local buckling, large plastic deformation of plates and tube, poor fire resistance and corrosion needs to be well investigated and considered. This study, however, is limited to the mechanical behavior of CFST column under static loading.

The focus of this paper is to investigate the accuracy of a fiber based model in predicting the behavior of CFST columns. Further, this paper also presents the results of three-dimensional nonlinear finite element analysis using 3D-NLFEA for comparison purposes. When predicting the full response of CFST columns, fiber-based model require less computational time than a full three-dimensional (3D) nonlinear finite element analysis. The fast execution time of the fiber-based approach makes it a convenient tool in design. Moreover, the method can be implemented to evaluate the nonlinear behavior of RC frames under static, cyclic or dynamic loads. However, in the fiber-based method, some analytical models are required to simulate the behavior of a three-dimensional structural element into two-dimensional (2D) sectional analysis.

In the proposed fiber based model, Attard and Setunge's (4) empirical constitutive model for the concrete material is used together with the elastic-perfectly plastic model for the steel tube. As highlighted the method is two-dimensional, hence the local buckling of the steel tube and the confinement effect to the concrete core could not be directly modeled. In the analysis, the local buckling of the steel tube is considered by using the effective yield strength based on Eurocode 4 (5). Furthermore, for circular columns, Eurocode 4 allows the inclusion of the confinement effect of the concrete core if the slenderness ratio and the eccentricity ratio are both less than 0.5. To predict the confining pressure of the concrete core, an inverse analysis is carried out by equating the peak axial load capacity of the fiber-based method with the Eurocode 4 prediction. Once the confining pressure is computed, the confining pressure is held constant and is used to predict the behavior of CFST columns. The predictions are then compared with both the experiments and the 3D Non-Linear FEA (3D-NLFEA).

This paper is organized into several sections. The first section was the introduction. The second section contains the formulation for the fiber based method and the Open Source software used during the development and computation. The third section covers a brief description of the constitutive model for the concrete and the steel tube materials. The fourth section discusses the inverse method to compute the confining pressure of CFST column. The fifth section contains the comparison with the experimental results and 3D Non-Linear FEA. The sixth section is the conclusion and possible future works.

2. Fiber based method

In the 2D sectional analysis using a fiber-based method, the section is discretized into smaller elements. In this study, the Constant Strain Triangle (CST) elements are used in which the evaluation of the axial stress and strain is at the center of CST element. The use of higher order elements (such as a Linear Strain Triangle) will increase the accuracy when there is a strain gradient. However, for simulating concentrically loaded CFST columns where all the strain in the elements is equal, there are no differences between the results obtained using the lower or higher order elements. In the analysis, displacement-based control load application is used as in the experimental setup. The fiber-based method developed in this paper can be used not only to evaluate regular/symmetric sections but also in evaluating irregular section. From the fiber-based analysis, the axial force (F_x) and moments in x and y directions (M_{xx} and M_{yy}) can be formulated as:

$$F = \sum_{i}^{nele} \sigma_i A_i \quad M_{yy} = \sum_{i}^{nele} \sigma_i A_i \left(y_i - \bar{y} \right) \qquad M_{xx} = \sum_{i}^{nele} \sigma_i A_i \left(x_i - \bar{x} \right) \tag{1}$$

where σ_i is the stress in each element; A_i is the area of each element; x_i and y_i are the center coordinate of each element in x and y directions, respectively; $\bar{x}$ and $\bar{y}$ are the centroid of the section in the x and y directions.

The developed code is written in C#.Net (6). The modelling and mesh discretization is prepared using SALOME 7.8.0 (7). The analysis results are then written in a .vtk format file which is accessible in ParaView (8, 9) inside the SALOME 7.8.0. An axial force versus axial strain is dynamically reported during the runtime and is plotted using GNUPlot 5.1.0. Figure 1 shows an example of mesh discretization and axial stress contour of CFST column using ParaView.

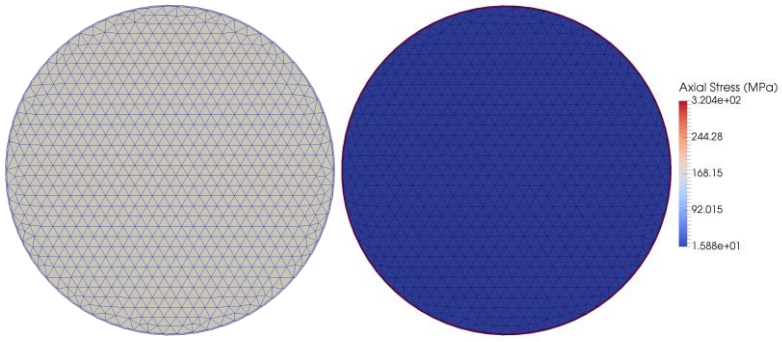

(a) (b)

Figure 1. (a) Mesh discretization of circular CFST column (b) Stresses in the CST elements for circular CFST column.

3. Constitutive models of the materials

The model of Attard and Setunge (4) is adopted for the concrete constitutive model which provides a good prediction of concrete material behavior for a wide range of concrete strength from normal (20 MPa) to a very high concrete strength (130 MPa). The constitutive model is classified as the empirical model where the stress is computed explicitly based on a given axial strain. The formulation for the stress-strain curves is based on the model of Sargin et. al. (10) and is given here as:

$$Y = \frac{AX + BX^2}{1 + CX + DX^2} \quad \text{where} \quad Y = \frac{f}{f_{cc}}, X = \frac{\varepsilon}{\varepsilon_{cc}} \quad \text{and} \quad \forall X \geq 0 \quad 0 \leq Y \leq 1 \tag{2}$$

where f is the axial stress at axial strain ε, f_{cc} is the axial peak stress at axial strain ε equal to ε_{cc}. A, B, C, D are constants that need to found using different boundary condition (see (4) for more detail).

The Attard and Setunge's (4) axial peak stress (f_{cc}) is:

$$\frac{f_{cc}}{f_c^{'}}=\left(\frac{f_r}{f_t}+1\right)^k \quad \text{with} \quad k=1.25\left[1+0.062\frac{f_r}{f_c^{'}}\right]\left(f_c^{'}\right)^{-0.21} \tag{3}$$

where f_c is uniaxial concrete compressive strength, f_r is the confining pressure and f_t is the uniaxial tensile strength of concrete. Note that the Attard and Setunge's (4) failure surface is extendable to the tension-compression region (11). For more detail and complete formulation, see (4).

The steel tube behavior is simulated by an elastic-perfectly plastic model. The program can also incorporate hardening, or softening modulus in the steel model. The longitudinal steel rebar, if present, is modeled as a discretized solid circle and their behavior can be predicted by similar constitutive models used for the steel tube.

4. Confining Pressure Estimation

In the fiber-based method, normally the confinement is estimated based on the strain compatibility between reinforcement ties and lateral strain of the concrete (12) and simple equilibrium requirement between ties and concrete core similar to the method in (13, 14). However, in CFST columns, the steel tube is under axial compression as well as circumferential stresses at the same time which reduces the steel tube capacity. In this study, confining pressure is back calculated by firstly computing the axial carrying capacity (P_{max}) of the CFST column using Eurocode 4 or directly adopting the data from the test results. In Eurocode 4, the axial carrying capacity of the CFST column is estimated as:

$$P_{max}=P_{steel}+P_{conc}=\eta_s A_s f_y+A_c f_c^{'}\left(1+\eta_c\frac{t}{d}\frac{f_y}{f_c^{'}}\right) \tag{4}$$

where η_s is the strength reduction coefficient for the steel tube, A_s is the cross-sectional area of the steel tube, f_y is the yield strength of the steel tube, A_c is the cross-sectional area of the concrete, f_c is the uniaxial compressive strength of the concrete, η_c is a coefficient enhancement of the concrete strength due to the confinement effect, t is the thickness of the steel tube and d is the outer diameter of the steel tube.

In Eurocode 4, the strength reduction coefficient (η_s) and the concrete enhancement due to the external confining devices (η_c) is computed based on the slenderness ratio (λ) and the ratio of the load eccentricity to the diameter of the specimen (e/d). The expressions for η_s and η_c are:

$$\eta_s=0.25\left(3+2\lambda\right)+\left(1-0.25\left(3+2\lambda\right)\right)\left(10e/d\right) \tag{5}$$

$$\eta_c=\left(4.9-18.5\lambda+17\lambda^2\right)\left(1-10e/d\right) \tag{6}$$

$$\lambda=\sqrt{\frac{\left(A_s f_y+A_c f_c^{'}\right)L^2}{\pi^2\left(EI\right)_{eff}}} \tag{7}$$

where L is the height of the specimen and $(EI)_{eff}$ is the effective stiffness of the columns. Please note that η_c is only considered if the slenderness ratio is less and equal than 0.5 and also if the ratio of the load eccentricity to the diameter of the specimen is less than 0.5.

Once P_{conc} is computed, the confining pressure is back calculated by simply equating the strength of confined concrete from Attard and Setunge (4) model with the Eurocode 4 confined concrete strength prediction as:

$$\left(1+\eta_c\frac{t}{d}\frac{f_y}{f_c^{'}}\right)=\left(\frac{f_r}{f_t}+1\right)^{k_1} \tag{8}$$

$$k_1 = 1.25\left(1 + 0.062\left(\frac{f_r}{f_c'}\right)\right)\left(f_c'\right)^{-0.21} \tag{9}$$

Obtaining a direct solution for the confining pressure from Eqns. (8) and (9) is rather difficult. Hence, an iterative numerical approach based on Regula-False method is adopted to find the confining pressure at the peak force level. Following the above method to compute the confining pressure, the predicted P_{Max} based on the fiber based method will be the same as the computed P_{max} using Eurocode 4. If P_{Max} is directly extracted from the test results, Equation (8) can be rewritten by replacing the left-hand side of the equation by confined core strength increase in the experiment. The axial force contribution of concrete (P_{Conc}) is then calculated by subtracting the axial force contribution of steel (P_{Steel}) from the total force of the specimen (P_{Max}). Dividing P_{Conc} with the area of concrete times the concrete uniaxial compressive strength will be the core strength enhancement in the experiment. In summary, Equation (8) can be rewritten as:

$$\frac{P_{Max} - P_{Steel}}{A_c f_c'} = \frac{P_{Conc}}{A_c f_c'} = \left(\frac{f_r}{f_t} + 1\right)^{k_1} \tag{10}$$

Confinement will be calculated by iteration from Equation (10) as well.

5. Comparisons and discussion of the fiber-based approach with the finite element analysis and the experimental results

Two experiments of CFST columns from Lai and Ho (15) are modeled to verify the proposed fiber-based approach. The first specimen is identified as CN0-1-114-30 in which the concrete compressive strength is 31.4 MPa with a modulus of elasticity of 19.7 MPa and the uniaxial axial peak strain of 0.0029. The second specimen is identified as CN0-1-114-80 with a concrete compressive strength of 79.9 MPa, a modulus of elasticity 30.7 MPa for concrete material and the uniaxial axial peak strain of 0.0036. Both specimens have the same geometry and material properties of the steel tube. The steel tube has an outer diameter of 111.5 mm, and the thickness of the steel tube is 0.96 mm. The uniaxial yield strength of the steel tube in tension is 370 MPa. The modulus of elasticity and the Poisson's ratio of the steel tube is 206 GPa and 0.29, respectively.

Using Eurocode 4, the axial load carrying capacity of CN0-1-114-30 and CN0-1-114-80 are 418.34 kN and 867.99 kN respectively while the confining pressure for CN0-1-114-30 and CN0-1-114-80 are estimated to be 1.027 MPa and 0.962 MPa respectively. If the confining pressure is computed based on maximum experimental axial load carrying capacity, the confining pressure for CN0-1-114-30 and CN0-1-114-80 are estimated as 2.148 MPa and 1.897 MPa, respectively. Since the confining pressure at peak stress is known, the fiber-based analysis is carried out by assuming a constant confining pressure throughout the loading steps. It is worth mentioning that, in the experimental results (15), after reaching the peak stress and during softening, the confining pressure is still increasing. Hence, it is expected that the load carrying capacity of the column in softening regions predicted from the fiber-based method is lower in comparison with the experimental results.

In addition to the fiber based method predictions, a three-dimensional non-linear finite element analysis of these two specimens are carried out using an in-house FEM program called (16) (3D-NLFEA). The constitutive model used for analysis in 3D-NLFEA is Piscesa's plasticity model (11, 17). The constitutive model for the steel material is Von-Mises criterion or a J_2 plasticity model with zero hardening modulus. In the 3D-NLFEA, the CFST column is modelled using 6,076 hexahedral elements with full integration. Both ends have fixed boundary conditions, and a displacement controlled loading scheme is considered. Figure 2 shows the 3D-NLFEA model of CN0-1-114-30, the hardening parameter, the confining pressure and the axial stress distribution for CFST column at the average axial strain equal to 0.016. The data contour is presented by showing the vertical cross section of the specimen.

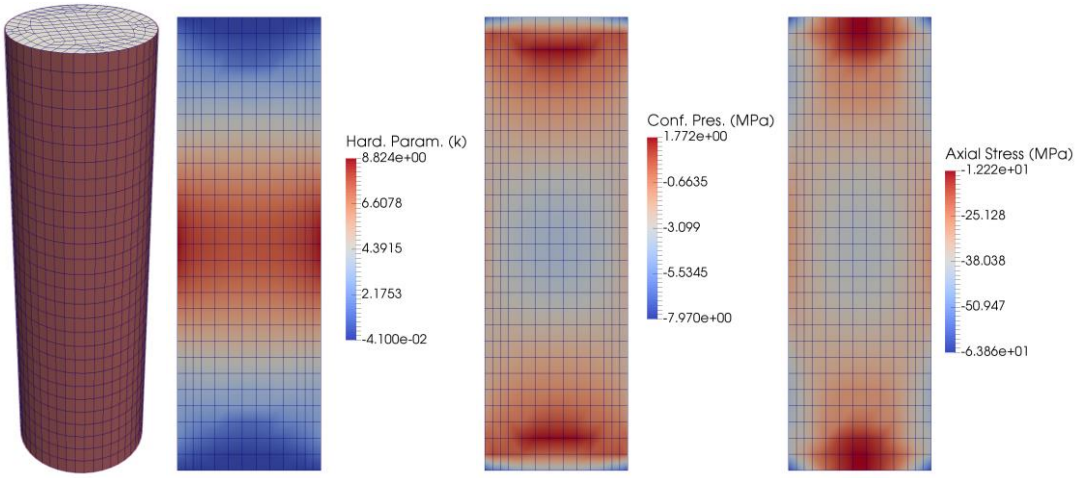

(a) (b) (c) (d)

Figure 2. a) 3D-NLFEA model of CN0-1-114-30 b) Hardening parameter c) Confining pressure (d) Axial stress. The contour is shown at the average axial strain equal to 0.016.

From Figure 2b, the hardening parameter has the highest value at the mid-height which clearly showing the localized region. The distribution of the confining pressure throughout the specimen is not constant with the regions near the platen having higher confining pressure compare to the region at the mid-height of the specimen (see Figure 2c). Figure 2d shows that the axial stress distribution at both end is lower than at the mid-height of the specimen. The lower value of the axial stress distribution at both ends is due to elastic unloading occurring at those regions. These phenomena could not be captured by using a 2D fiber-based model.

Figure 3 and 4 show the comparisons of the axial load versus the axial strain between the fiber-based method, 3D-NLFEA and the experimental results for CN0-1-114-30 and CN0-1-114-80, respectively. Figure 3 shows that the predicted peak axial load carrying capacity using Eurocode 4 (418.34 kN) is lower than the value obtained from the 3D-NLFEA (467.12 kN) and the experimental result (479 kN). However, if the concrete strength enhancement is calculated based on Eqn.(10), the overall predicted response using the fiber-based method is closer to the 3D-NLFEA. It is worth highlighting that both the 3D-NLFEA and fiber based method show lower axial capacity during softening after the peak load. Figure 4 also shows the predicted peak axial load carrying capacity using Eurocode 4 (867.99 kN) is lower than the value obtained from the 3D-NLFEA (997.34 kN) and the experimental result (955 kN). The predicted axial capacity of fiber based model during softening is much lower than 3D-NLFEA and the test results. The lower softening response from the fiber based analysis could be attributed to the constant confining pressure assumption which is more pronounce in high strength concrete specimen. From the discussion above, 3D-NLFEA gives more accurate results and the use of fiber-based model should be improved in the future for CFST column made of high strength concrete.

To study size effect phenomena in the 3D-NLFEA analysis, axial shortening of the column is recorded in two ways. In the first method, the column shortening is a total height shortening between platens thus the end regions near the platens, which are elastically unloading, are also included in the computed average axial strain. While in the second method, column shortening in a distance of two times of the diameter in the middle of the column height is used to compute the average axial strain. Thus, in the second method, the region near the platen is not included when computing the axial strain. The load-strain response by using the first measurement has steeper softening slopes than the second measurement (see Figure 3 and 4) which clearly shows that the 3D-NLFEA can capture the size effect in the analysis. Hence, it is important to note that when comparing the analysis with the experiments, the location of the measurement points is important.

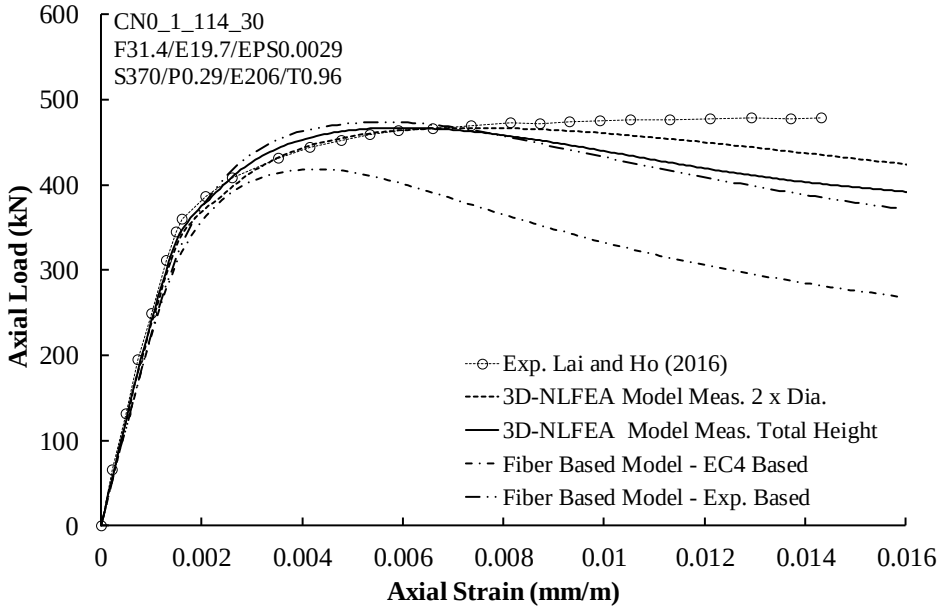

Figure 3. Comparisons of the model with 3DNLFEA and experimental results for CN0_1_114_30 specimen.

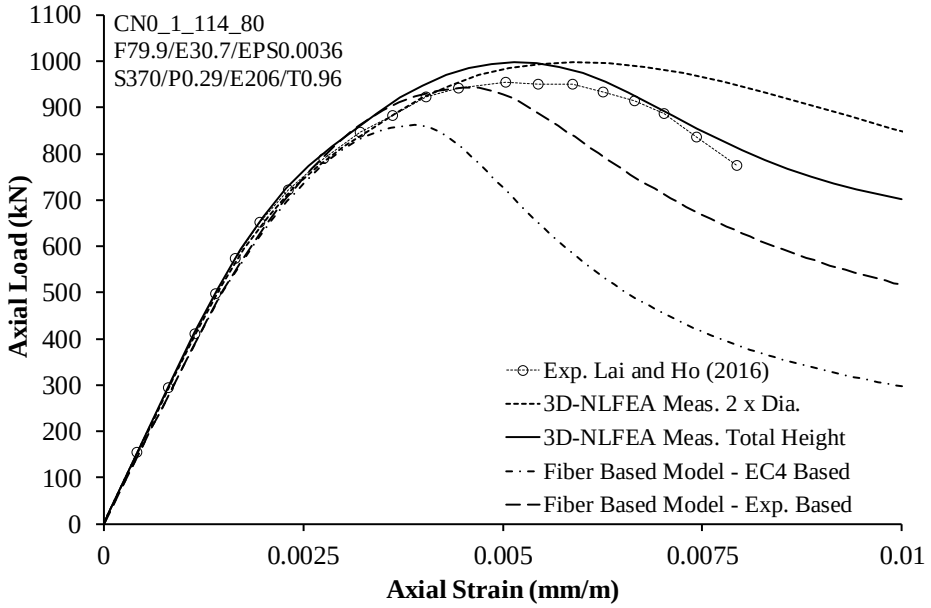

Figure 4. Comparisons of the model with 3DNLFEA and experimental results for CN0_1_114_80 specimen.

6. Conclusion and future work

This paper investigated the performance of the fiber based method in predicting the behavior of concrete filled steel tube (CFST) columns. The use of the fiber-based method is extremely fast and can be extended to a larger scale non-linear analysis such as a non-linear frame analysis. Although the comparisons shown in this paper were limited, the results showed that the use of fiber-based method tended to underestimate the load-deformation response of the CFST columns. There was two main reasons highlighted; the first reason was that the predicted axial load carrying capacity, which was based on Eurocode 4, was lower than the experiments and the second was because of the constant confining pressure assumption throughout the analysis. The first problem could be rectified by using

the peak load from the test results, however, experimental data was not always available during design and thus a more robust method to estimate the confinement that should be carried out. On the other hand, the use of full 3D-NLFEA showed an excellent prediction because of the ability of the constitutive model to capture not only the peak response but also the softening response of the selected specimen.

Furthermore, the size effect phenomena in the load-deformation response using 3D-NLFEA is discussed briefly. The future works are focused on improving the formulation to predict the axial load carrying capacity of CFST column and using a more advanced concrete constitutive model which involves the inclusion of the size effect (18) and the lateral strain model (19). The inclusion of the size effect allows the fiber-based method to account for the localized region in the specimen and thus affecting the load-deflection behavior when softened. On the other hand, by using the lateral strain model, the estimate of the confining pressure is more accurate. Further, in the future, a non-circular section and complex configuration of the CFST with steel rebar also worth to be investigated.

7. References

[1] Gjørv O. High strength concrete. Developments in the Formulation and Reinforcement of Concrete. 2008:79-97.
[2] Foster SJ. On behavior of high-strength concrete columns: cover spalling, steel fibers, and ductility. Structural Journal. 2001;98(4):583-9.
[3] Foster SJ, Liu J, Sheikh SA. Cover spalling in HSC columns loaded in concentric compression. Journal of Structural Engineering. 1998;124(12):1431-7.
[4] Attard M, Setunge S. Stress-strain relationship of confined and unconfined concrete. ACI Materials Journal. 1996;93(5).
[5] EN C. 1-1, Eurocode 4: Design of composite steel and concrete structures. Part; 1994.
[6] Microsoft. Visual C# Ver. 6.0. https://www.visualstudio.com/. 2015.
[7] CEA/DEN, EDF_R&D, OPEN_CASCADE. SALOME - The Open Source Integration Platform for Numerical Simulation. http://www.salome-platform.org/. Ver. 7.8.0 ed 2016.
[8] Ahrens J, Geveci B, Law C, Hansen C, Johnson C. 36-ParaView: An End-User Tool for Large-Data Visualization. The Visualization Handbook. 2005:717.
[9] Ayachit U. The paraview guide: a parallel visualization application. 2015.
[10] Sargin M. Stress-strain relationships for concrete and the analysis of structural concrete sections: Solid Mechanics Division, University of Waterloo Waterloo, ON, Canada; 1971.
[11] Piscesa B, Attard M, Samani A, Tangaramvong S. Plasticity Constitutive Model for Stress-Strain Relationship of Confined Concrete. Structural Journal. 2017;114(02):361-71.
[12] Samani AK, Attard MM, Foster SJ. Ductility in concentrically loaded reinforced concrete columns. Australian Journal of Structural Engineering. 2015:1-14.
[13] Sheikh S, Uzumeri S. Analytical model for concrete confinement in tied columns. Journal of the Structural Division. 1982;108(12):2703-22.
[14] Sheikh S, Uzumeri S. Strength and ductility of tied concrete columns. Journal of the Structural Division. 1980;106(5):1079-102.
[15] Lai M, Ho J. A theoretical axial stress-strain model for circular concrete-filled-steel-tube columns. Engineering Structures. 2016;125:124-43.
[16] Piscesa B, Attard MM, Samani AK. Three-dimensional Finite Element Analysis of Circular Reinforced Concrete Column Confined with FRP using Plasticity Model. Procedia Engineering. 2017;171:847-56.
[17] Piscesa B, Attard MM, Samani AK. A lateral strain plasticity model for FRP confined concrete. Composite Structures. 2016;158:160-74.
[18] Samani A, Attard M. A Stress-Strain Model for Uniaxial and Confined Concrete under Compression. Engineering Structures. 2012;41:335-49.
[19] Samani AK, Attard MM. Lateral Strain Model for Concrete under Compression. ACI Structural Journal. 2014;111(1-6).